

## Local representation of the exchange nonlocality in $n$ - $^{16}\text{O}$ scattering

G. H. Rawitscher and D. Lukaszek

*Physics Department, University of Connecticut, Storrs, Connecticut 06269*

R. S. Mackintosh and S. G. Cooper

*Physics Department, The Open University, Milton Keynes, United Kingdom*

(Received 7 December 1992)

The nonlocal Schrödinger equation is solved rigorously in a microscopic folding model, incorporating both direct and knock-on exchange potentials, for  $n$ - $^{16}\text{O}$  scattering at laboratory energies of 20 and 50 MeV. The model uses the complex and density dependent  $n$ - $n$  interaction of N. Yamaguchi *et al.*, uses harmonic oscillator wave functions for the bound nucleons, and calculates the scattering wave function for this nonlocal problem using a Bessel-Sturmian expansion method incorporating correct boundary conditions. All spins are neglected. The local phase-equivalent potential is obtained from the scattering matrix elements at a given energy by using the iterative perturbative inversion method. This representation allows comparison between the microscopic model and a phenomenological potential, showing good agreement for the local real part of the potential at 20 MeV. From the ratio of the wave functions for the nonlocal potential and for the potential calculated by inversion, a Perey damping factor (PDF) is obtained which is of similar form to the well-known Perey-Buck prescription for the PDF for a Gaussian nonlocality of the conventional range of 0.85 fm. The significance of these results for distorted wave Born approximation calculations is discussed.

PACS number(s): 24.10.Ht, 25.40.Dn

### I. INTRODUCTION

The optical potential which describes the elastic scattering of a nucleon from a target nucleus is nonlocal and, in principle, very complicated. The dynamic polarization of the nucleus during the scattering process is one of the sources of the nonlocality, and the knock-on exchange mechanism is another. Since the nonlocalities of the optical potential are not known exactly, it is the general practice to use instead of local optical potential when evaluating a nuclear reaction by means of the distorted wave Born approximation (DWBA). As is well known, the wave functions for a nonlocal potential are different from those of a local equivalent potential (LEP), [1] and it is common practice to correct for this difference by the use of a multiplicative factor, called the Perey damping factor (PDF). The most commonly used PDF is the one introduced many years ago by Perey and Buck [1,2], but this factor is known to be valid only if the nonlocality is of a Gaussian form.

The need to investigate the form of the PDF which corresponds to a particular nonlocality has regained renewed importance in view of the study of the shell-model occupation numbers by means of the  $(e, e'p)$  reaction. It is desirable to determine these numbers to an accuracy of better than 10%, yet their values vary by more than 20% depending on the type of the optical model used to describe the distortion of the knocked-out nucleon [3]. Recent advances in calculating microscopic nonlocal optical potentials from effective  $n$ - $n$  interactions makes it less well justified to use phenomenological potentials to obtain the distorted wave functions needed in the calculation of  $(e, e'p)$  or  $(p, p')$  reactions. Until such nonlocal

optical potentials are in wide use, it is of interest to examine the local equivalent optical potentials and their corresponding PDF's as a preferred meeting ground between theory and experiment.

The aim of this paper is to rigorously study the effect of the knock-on exchange nonlocality and at the same time obtain a LEP by a method of inversion. Our example refers to  $n$ - $^{16}\text{O}$  scattering at low energy (20 and 50 MeV). Our LEP is  $L$  independent, yet it reproduces the scattering matrix elements to high precision. We thereby provide a result against which the commonly used approximate methods for obtaining LEP's for the knock-on exchange term can be compared. Among the latter exist the energy density approximation method [4,5] and another one developed by Horiuchi [6], based on the Wentzel-Kramers-Brillouin (WKB) approximation. We also compare the nonlocal and corresponding local wave functions in order to investigate how well their ratio is given by the conventional Perey-Buck result [2].

We obtain the exact solution for the nonlocal potential by a Fourier-Sturmian expansion technique [7], which for the case of a local potential has been found to converge very well [8] and which has been generalized to the nonlocal case [9]. We obtain the LEP by the iterative perturbative (IP) inversion method [10], which uses as input information the scattering matrix elements for all  $L$  values at a given energy. The resulting LEP is phase equivalent to the nonlocal potential, i.e., the wave functions asymptotically are nearly the same, while at small distances they differ. As implemented, this inversion method avoids the presence of spurious waviness in the potential by obtaining the solution of an overdetermined system of equations by means of the singular value decomposition method.

Some aspects of our investigation have been studied previously. Lassaut and Vinh Mau [11] have calculated  $n$ - $^4\text{He}$  elastic scattering phase shifts from various effective nucleon-nucleon interactions and obtained approximate LEP's for the exchange terms. Fiedeldey, Sofianos, and Allen [12], using a particular set of  $n$ - $^4\text{He}$  phase shifts from Ref. [11], obtained a real LEP using their inversion technique and examined the corresponding Perey factors. Keneko, LeMere, and Tang [13] have employed a real nucleon-nucleon potential to construct the direct and exchange pieces of the nucleon-nucleus optical potential, while the imaginary part of this potential was taken from previously determined phenomenological local optical potentials. They obtain good fits to the experimental cross sections and polarizations, thus showing that the exchange nonlocality based on the knock-on term alone (this is their model K method) is compatible with experiment for nuclei which have more than 12 nucleons. Their LEP's use the WKB methods developed by Horiuchi [6], but they do not investigate the PDF's. The work of Horiuchi on the interaction potential between two heavy ions, based on the microscopic resonating-group-method formulation, is also to be noted [14]. Recently, IP inversion has been used to directly calibrate the resonating-group-method Wentzel-Kramers-Brillouin (RGM-WKB) approach [15]. An older study by Owen and Satchler [16] is similar to that of Ref. [13] in that the imaginary potential is also local and phenomenological. They obtain a LEP by searching for the parameters of a conventional Woods-Saxon-type optical potential which gives the same cross section as that of the nonlocal potential, and they compare the local and nonlocal wave functions. The effect of the exchange nonlocality has also been investigated by Bauhoff, von Geramb, and Pállá [17]. Their study is similar to ours in that the nonlocal optical potential is based on folding a complex density-dependent effective interaction over the target nucleon distribution, but differs from ours in that the inversion of the nonlocal into a LEP is based on the Wronskian method [18] and hence is  $L$  dependent.

The main difference of our study from the ones mentioned above is that we combine the following features into the same study: We employ a complex effective  $n$ - $n$  interaction [19], include the knock-on exchange term rigorously to calculate the  $n$ - $^{16}\text{O}$  phase shifts, use an inversion technique [10] to transform the phase shifts into an  $L$ -independent local potential, and rigorously compare the wave functions. The effective  $n$ - $n$  interaction we use is still much simpler than the sophisticated ones which have been used recently [20] in order to calculate elastic nucleon-nucleus cross sections. However, the cited calculations are for energies where the impulse approximation might be expected to work. We are concerned with much lower energies which are important in making the link between scattering and bound state potentials. At such energies one must employ an effective potential rather than the free  $T$  matrix.

The inversion method used to obtain the local equivalent potential from the scattering matrix elements (SME's) [10] is an iterative, perturbative method, which has had numerous applications. It has been used to ex-

amine the nonlocality due to nuclear dynamic polarization and obtain the corresponding Perey damping factors [21]. It has also been used to obtain local potentials for  $p$ - $^4\text{He}$  scattering from  $R$ -matrix phase shifts [22] and also for heavy-ion scattering [23]. A user's manual describing the inversion code is available [24].

## II. FORMALISM

In the presence of exchange, the Schrödinger equation becomes nonlocal. In the Hartree-Fock approximation, the local potential is obtained by folding the microscopic  $n$ - $n$  interaction over the occupied single-particle states  $\varphi_a$

$$V_H(r_0) = \sum_a \int \varphi_a(\mathbf{r}_1)^* v_{\text{dir}}(|\mathbf{r}_1 - \mathbf{r}_0|) \varphi_a(\mathbf{r}_1) d^3 r_1, \quad (2.1a)$$

and the exchange kernel for the knock-on exchange process is given by

$$K(\mathbf{r}_0, \mathbf{r}'_0) = - \sum_a \varphi_a(\mathbf{r}_0)^* v_{\text{exch}}(|\mathbf{r}_0 - \mathbf{r}'_0|) \varphi_a(\mathbf{r}'_0). \quad (2.1b)$$

The density dependence of the microscopic  $n$ - $n$  effective interaction is not explicitly indicated in the above, but is taken into account in what follows. Only the central part of the  $n$ - $n$  interaction is included here. Since the latter is rotationally invariant, the exchange kernel can be projected onto each partial wave with angular momentum number  $L$ . The result is denoted as  $K_L(r_0, r'_0)$ , and an analytical expression is given below.

The central part of the  $n$ - $n$  interaction is given [19] by a sum over three Gaussian terms of the form  $V_i \exp[\alpha_i r^2]$ , each multiplied by a factor  $\{1 + A_i k_F + B_i k_F^2\}$ , where  $k_F$  is the density-dependent local Fermi momentum. For the nucleus  $^{16}\text{O}$ , we approximate  $k_F(R)$  by a sum over two Gaussians in  $R^2$  and likewise for  $k_F^2$ . As a result, the  $n$ - $n$  interaction of Ref. [19] can be represented as a sum of terms of the form

$$V \exp[-\alpha r^2 - \beta_F R^2], \quad (2.2)$$

where  $r$  is the distance between the two interacting nucleons and  $\mathbf{R}$  is the position of their center of mass relative to the center of the nucleus. The quantities  $V$  and  $\alpha$  are obtained from the tables in Ref. [19], and the parameters  $\beta_F$  arise from the approximation of the  $R$  dependence of  $k_F$  or  $k_F^2$  in terms of two Gaussian functions of  $R^2$ . For the single-particle states in  $^{16}\text{O}$ , we use harmonic oscillator wave functions in the absence of spin-orbit couplings. Their radial parts contain powers of  $r_1$  times  $\exp[-\beta_a r_1^2]$ . With the assumptions described above, one obtains for the partial wave exchange kernel  $K_L$  for each term of the  $n$ - $n$  interaction given by Eq. (2.2) the result

$$K_L(r_0, r'_0) = 4V(2\beta_a)^{3/2}\pi^{-1/2}r_0r'_0 \exp[-(\beta_a + \alpha_P)(r_0^2 + r'^2_0)] \left\{ i_L(z) + \frac{4\beta_a r_0 r'_0}{2L+1} [Li_{L-1}(z) + (L+1)i_{L+1}(z)] \right\}. \quad (2.3)$$

In the above,  $z = 2r_0r'_0\alpha_M$ ,  $\alpha_P = (\alpha + \beta_F/4)$ ,  $\alpha_M = (\alpha - \beta_F/4)$ , and  $i_L(z)$  is a spherical modified Bessel function defined in [25]. The final result for  $K_L$  is a superposition of expressions of the type of Eq. (2.3), for all the components (2.2) of the exchange part of the effective  $n$ - $n$  interaction. It is clear that  $K_L$  is indeed  $L$  dependent and of a complicated nature. In Figs. 1 and 2 we illustrate the real and imaginary parts of the exchange kernel  $K_L(r_1, r_2)$  for the  $n$ - $^{16}\text{O}$  interaction at an incident energy of 20 MeV for two values of the angular momentum  $L$ . The magnitude of the real part of  $K_L$  decreases with  $L$ , as can be seen from the smaller scale of the vertical axis for the  $L = 3$  result. For the imaginary part, the height of the ridges on either side of the trough decreases gradually with  $L$ .

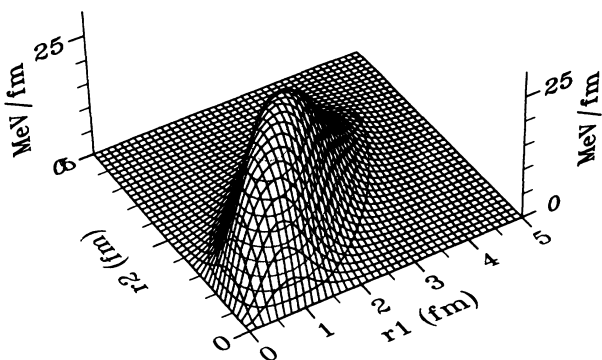
Our method of solving the nonlocal Schrödinger equa-

tion consists in expanding the (unknown) scattering wave function  $\mathcal{F}_L(r)$  for each partial wave  $L$  in a basis set of (known) Bessel-Sturmian functions  $\phi_{Lj}(r)$ ,  $j = 1, 2, \dots, M$  [7,8]. One obtains linear algebraic equations for the expansion coefficients, which require the calculation of matrix elements of the interaction between Sturmian basis states. In the presence of the exchange terms, this procedure can be generalized [9] and leads to the calculation of direct and exchange matrix elements of the type

$$V_{jj'} = \sum_a \langle \varphi_a(\mathbf{r}_1) \phi_{Lj}(\mathbf{r}_2) [v_{\text{dir}} \varphi_a(\mathbf{r}_1) \phi_{Lj'}(\mathbf{r}_2) - v_{\text{ex}} \varphi_a(\mathbf{r}_2) \phi_{Lj'}(\mathbf{r}_1)] \rangle.$$

Since the potentials and bound state wave functions are of the Gaussian form and the Sturmian functions are known spherical Bessel functions, it is possible to evaluate all the matrix elements analytically [9].

Real Part,  $L=0$  20 MeV



Real Part,  $L=3$  20 MeV

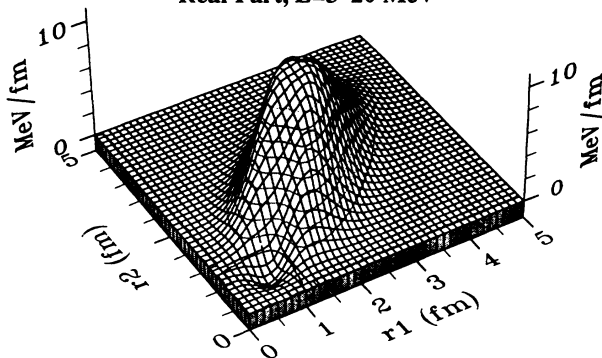
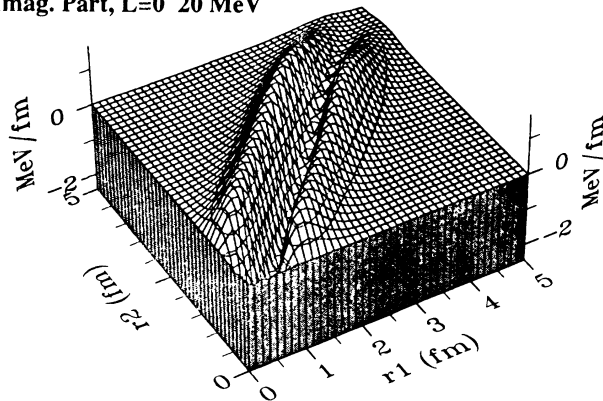


FIG. 1. Real part of the exchange kernel  $K_L(r_1, r_2)$ , defined by Eq. (2.3) for the  $n$ - $^{16}\text{O}$  interaction at an incident energy of 20 MeV. The microscopic  $n$ - $n$  interaction was taken from Ref. [19], with the imaginary part reduced by a factor of 0.6. The values of the angular momentum  $L$  are indicated. The change in the vertical scale between the top ( $L = 0$ ) and bottom parts ( $L = 3$ ) of the panels are to be noted.

Imag. Part,  $L=0$  20 MeV



Imag. Part,  $L=3$  20 MeV

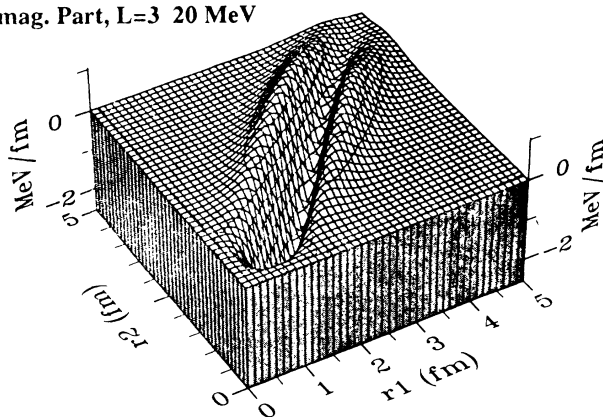


FIG. 2. Similar to Fig. 1 for the imaginary part of  $K_L(r_1, r_2)$ .

### III. RESULTS FOR THE POTENTIAL

Unless otherwise stated, the imaginary part of the microscopic  $n$ - $n$  interaction [19] is reduced by a factor of 0.6. The size of this reduction is comparable to the reduction used by other authors for  $n$ - $^{40}\text{Ca}$  scattering [19] and for  $n$ - $^{16}\text{O}$  scattering [26]. The size of the matching radius  $R$  used in the determination of the Sturmian wave numbers  $K_{Lj}$  is 15 fm. The harmonic oscillator wave function decay constant  $\beta_a$  for the nucleus of  $^{16}\text{O}$  has the value of  $0.165\text{ fm}^{-2}$ . It is determined so that the rms radius of the charge distribution of  $^{16}\text{O}$  agrees with the experimental [27] value 2.70 fm. (The rms value of the proton's charge distribution is taken equal to 0.8 fm.) The size of the Sturmian basis  $M$  is 25, which suffices for an accuracy of four significant figures.

The results for the elastic scattering matrix elements (SME's) at an incident laboratory energy of 20 MeV are shown in Fig. 3, and the corresponding elastic cross section is shown in Fig. 4. The phenomenological optical-model fit uses the parameters of Petler *et al.* [26], with the spin-orbit potential set to zero. Considering that the theoretical calculation has only one free parameter (the strength of the microscopic imaginary potential), the agreement with the data is encouraging. The potential  $V_{\text{inv}}$ , reproducing the theoretical SME's, is shown in Fig. 5 by the solid lines. Inversion allows us to deduce that the nonlocal folding model based on the complex effective Gaussian (CEG) potential [19] gives a good representation of the real part of the local phenomenological optical potential, but a somewhat poorer representation of the imaginary part. Specifically, the imaginary part of  $V_{\text{inv}}$  has a considerably larger volume component than the best phenomenological optical potential. The direct part of the theoretical Hartree potential, obtained from

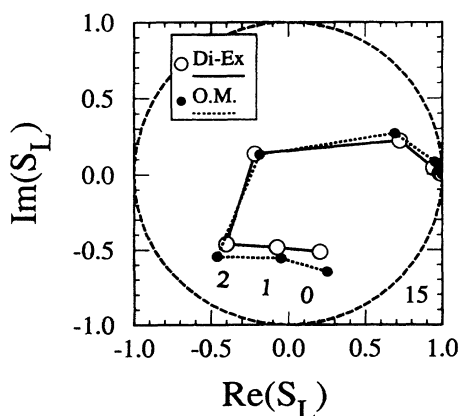


FIG. 3. Argand diagram of the elastic scattering matrix elements (SME's) for  $n$ - $^{16}\text{O}$  scattering for an incident laboratory energy of 20 MeV. The open circles represent the results of the microscopic theory including exchange. The microscopic  $n$ - $n$  interaction is the same as described in Fig. 1. The solid circles represent the optical-model results, employing the parameters of Petler *et al.* [26]. All spin-orbit potentials were set to zero. The first three values of the angular momentum number  $L$  are indicated.

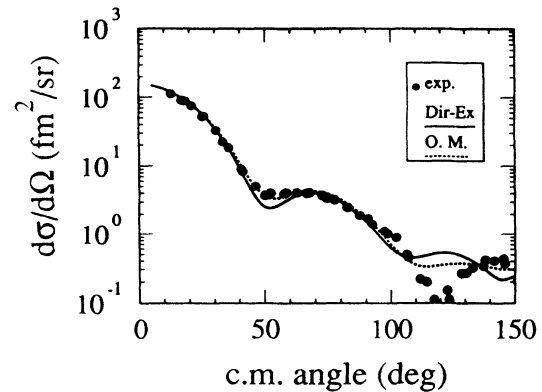


FIG. 4. Elastic cross sections obtained with the SME's shown in Fig. 3. The solid and dashed curves represent, respectively, the theoretical and phenomenological results; the experimental points are from Ref. [26]. Thirteen partial waves were used for the cross section calculation.

Eq. (2.1a), is illustrated by the dotted lines in Fig. 6. The difference between the dotted and solid lines is the contribution of the exchange potential, which is seen to be large (about half the total). This large size of the effect of the exchange potential is consistent with the magnitude of the exchange kernel, illustrated in Fig. 1.

A local approximation  $U_{\text{ex}}^1(r_0)$  to the exchange potential, based on Sinha's expression [5]

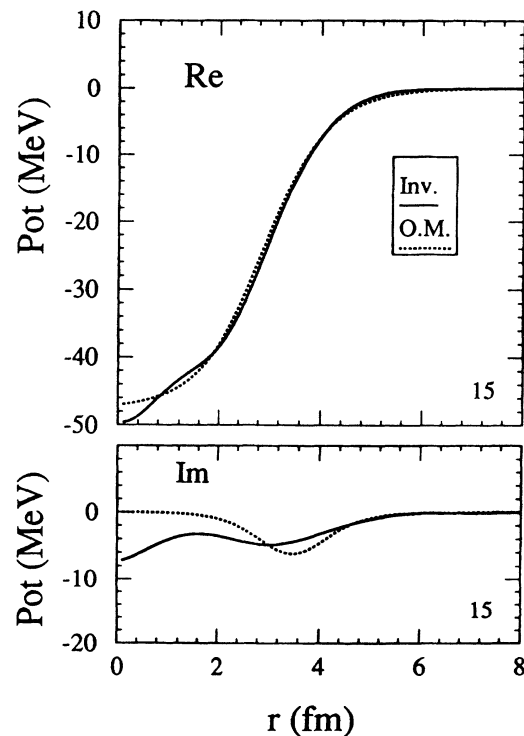


FIG. 5. Comparison of the inversion potential (solid lines) with the optical model of Ref. [26] (dotted lines), for  $n$ - $^{16}\text{O}$  scattering at 20 MeV. The real and imaginary parts are shown in the top and bottom panels, respectively. The corresponding SME's are illustrated in Fig. 3 for the first seven partial waves.

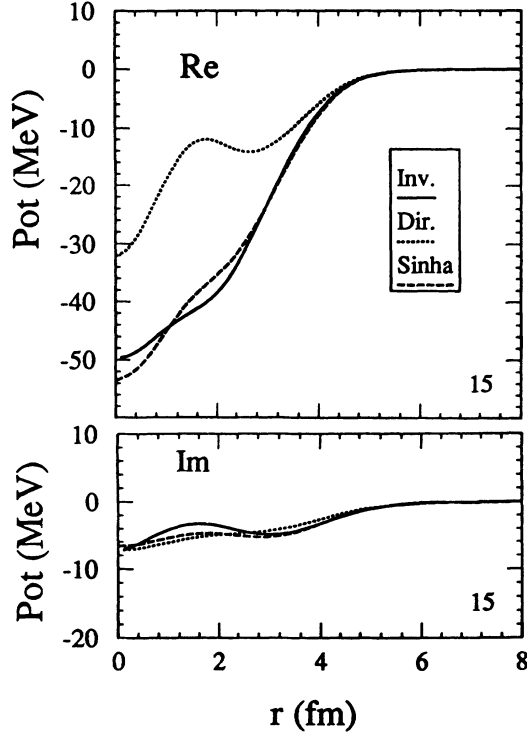


FIG. 6. Dotted lines show the direct part of the  $n$ - $^{16}\text{O}$  potential at 20 MeV, defined in Eq. (2.1a). The dashed lines represent an approximation to the direct plus exchange potentials, based on Sinha's method, defined in Eq. (3.1). The solid lines represents the inversion potential. One can see that nearly half of the real part of the total potential is due to exchange effects.

$$U_{\text{ex}}^l(r_0) = \int \rho(\mathbf{r}_0 + \mathbf{s}, \mathbf{r}_0) v_{\text{ex}}(\mathbf{s}, \mathbf{R}) [\sin(ks)/ks] d^3s, \quad (3.1)$$

was also obtained. Here  $k$  is the local wave number  $k^2(r_0) = (2m/\hbar^2)[E - U(r_0)]$ ,  $U$  is taken as the real part of the phenomenological optical potential,  $\mathbf{R} = \mathbf{r}_0 + \mathbf{s}/2$  is the center-of-mass position of the two interacting particles, and  $\rho(r_1, r_0)$  is the two-body density obtained from the harmonic oscillator wave functions in  $^{16}\text{O}$ . The sum of the direct potential (dotted lines) plus Sinha's approximation to the exchange potential is shown by the dashed lines in Fig. 6. The good agreement between the Sinha's LEP and our inversion potential indicates that both LEP's belong to the same family of optical potentials, and their difference is an indication of the reliability of Sinha's procedure.

The real part of the inversion potential is not very sensitive to the imaginary part of the microscopic  $n$ - $n$  interaction. This can be shown by changing the imaginary reduction factor of the microscopic  $n$ - $n$  interaction from 0.7 to 0.6. The change in the real part of  $V_{\text{inv}}$  was not visible in a graph showing the two potentials, while the imaginary part changed by a factor proportional to the change from 0.7 to 0.6. The inversion potential is very sensitive to the density dependence of the  $n$ - $n$  interaction. This can be seen by changing the density of

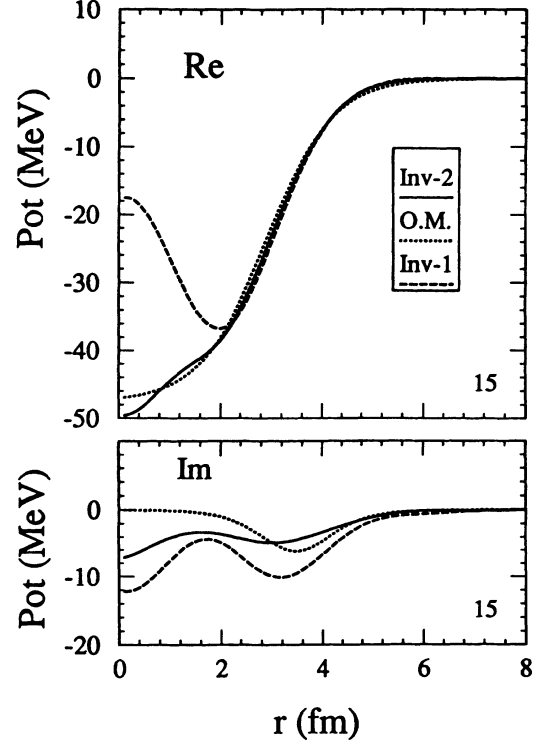


FIG. 7. Sensitivity of the inversion potential to the nuclear density. For the dashed lines the density in  $^{16}\text{O}$  is represented by a single Gaussian given by Eq. (3.2), while for the solid lines the density is close to the true one, as given by the harmonic oscillator single-particle description without spin. The dotted lines illustrate the phenomenological optical model of Ref. [26].

the nucleon distribution in  $^{16}\text{O}$  from the one given by the harmonic oscillator shell-model wave functions (it has a maximum at 1.231 fm) to that of a simple Gaussian of the form

$$\rho(r) = N \exp(-2\beta r^2), \quad (3.2)$$

which has the maximum at  $r = 0$  and assumes that all  $^{16}\text{O}$  nucleons in are in the  $s$  state. The resulting inversion potential acquires a repulsive "hump" near the center of the nucleus, as is illustrated in Fig. 7. Such repulsive humps were also observed [11] to occur in  $n$ - $^4\text{He}$  scattering when density-dependent microscopic potentials were used.

The energy dependence of the inversion potential is illustrated in Fig. 8. As the energy is changed from 20 to 50 MeV, the real potential becomes less deep and the imaginary becomes more volume and less surface, all in agreement with phenomenological expectations.

#### IV. RESULTS FOR THE WAVE FUNCTIONS

The comparison between the nonlocal and local wave functions is illustrated in Figs. 9 and 10. The nonlocal radial wave function is obtained from the Sturmian

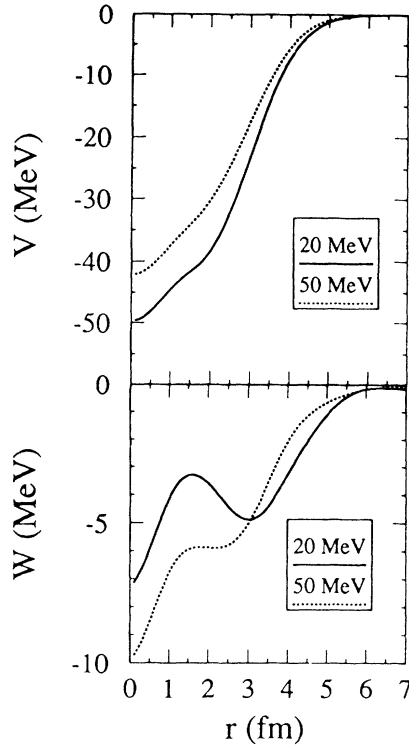


FIG. 8. Energy dependence of inversion potential for  $n^{-16}\text{O}$  scattering. The solid and dashed lines represent the 20 and 50 MeV results, respectively. The top and bottom panels represent the real and imaginary parts of these potentials, respectively.

method of solving the nonlocal Schrödinger equation, and the local wave function results from the local potential  $V_{\text{inv}}$ . The ratio between the absolute values of two “total” wave functions, summed over all partial waves, is denoted as the “total” Perey damping factor. It is illustrated in Fig. 9 as the ratio of the total nonlocal and total local wave functions. It is clear from the figure that the ratio of the two wave functions falls to about 0.86% over much of the nuclear volume, but rises to about 0.92 near the center of the nucleus and to unity toward the surface of the nucleus. Plots of the total Perey damping factor, such as Fig. 9 and also shown previously [22–24], are useful because they reveal details otherwise difficult to spot, such as the central “bump,” which would be absent if the conventional Perey-Buck PDF were valid. Also, the approximate spherical symmetry, evident in Fig. 9, is absent in the case that the nonlocality is due to channel coupling [22].

It is also possible to compare the nonlocal ( $nl$ ) and the local ( $l$ ) wave functions, described above, for each partial wave  $L$ , by means of the ratio  $F_L(r) = \mathcal{F}_L^{(nl)}(r)/\mathcal{F}_L^{(l)}(r)$ . Since the zeros of the two functions do not generally occur at exactly the same position, this ratio becomes very large near the zeros of the local wave function, thus making the plot for *all* values of  $r$  not very informative. This difficulty is circumvented by choosing only the maximum or minimum values of each wave function for calculating their ratio. The maxima of the absolute values of the

real (imaginary) parts of the two wave functions occur approximately at the same radial distances, and hence their ratio can be plotted at these discrete values of  $r$ , as is done in the right (left) panels of Fig. 10. The plot includes the points for all values of  $L$  from 0 to 2. The solid (open) symbols represent the ratios for an energy of 20 (50) MeV. The solid lines show the Perey-Buck result [2] for the damping factor for a nonlocality range of  $\beta = 0.85$  fm, which is the standard value accepted in the literature. For convenience the formula is repeated here:

$$F(r) = [1 - (2m/\hbar^2)(\beta/2)^2 V_N(r)]^{-1/2}. \quad (4.1)$$

The real part of the optical model of Ref. [26] was used for  $V_N$  in the equation above for the 20 MeV (dashed)

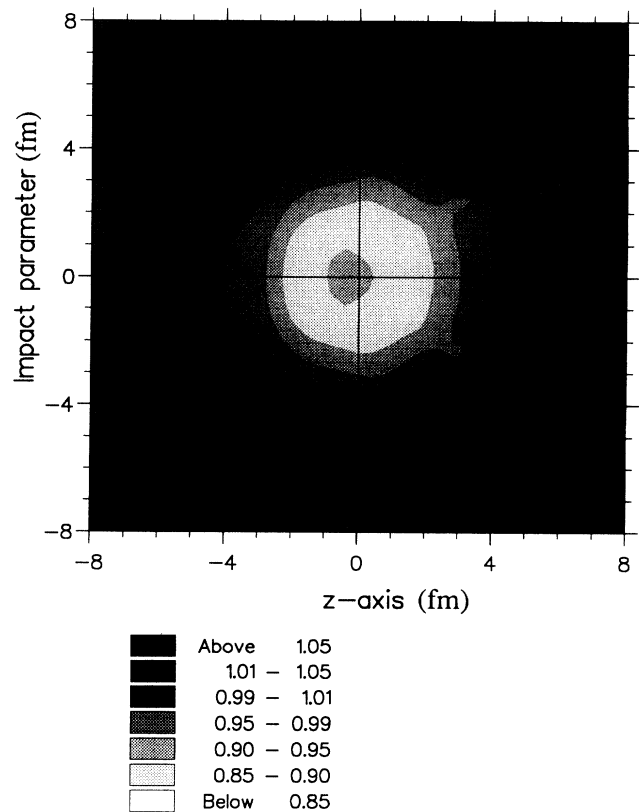


FIG. 9. Contour plot of the “total” Perey damping factor as a function of the impact parameter and the distance along the  $z$  axis for  $n^{-16}\text{O}$  scattering at 20 MeV. This is the ratio of the absolute value of two “full” (summed over all partial waves) wave functions. The wave function in the numerator is the exact nonlocal one (with exchange); the wave function in the denominator corresponds to the local inversion potential. Near the center of the nucleus, this ratio lies between 0.90 and 0.95; in the next region, which is spread over most of the nuclear volume, the ratio is between 0.85 and 0.90. In the next two layers, it rises from between 0.90 and 0.95 to between 0.95 and 0.99. Outside of the nucleus, with the exception of a few bands at the right, the value of the ratio is between 0.99 and 1.01. The bands are due to the cumulative effect of a slight mismatch error in the asymptotic value of the wave functions.

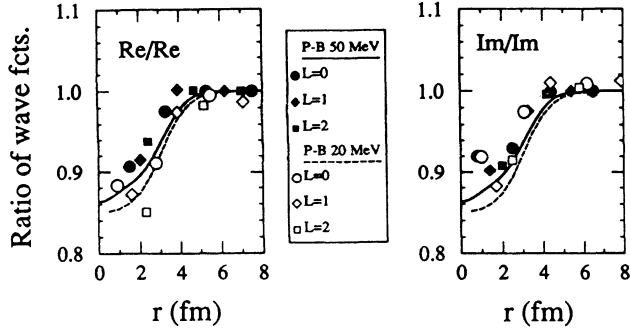


FIG. 10. Ratio of partial wave functions, at their maxima or minima, plotted at the discrete radial positions where the extrema occur, for  $n\text{-}^{16}\text{O}$  scattering. The wave function in the numerator is the exact nonlocal one (with exchange); the wave function in the denominator corresponds to the local inversion potential. The ratio of the real parts of these wave functions is displayed in the left panel, that of the imaginary parts in the right panel. The solid symbols represent the ratios at an incident energy of 50 MeV, the open ones at 20 MeV. The shapes of the symbols correspond to the different angular momenta  $L$ , as indicated. The solid line and dashed lines represent the conventional Perey-Buck damping factors, given by Eq. (4.1) for 50 and 20 MeV, respectively. Only the real parts of the inversion potentials were used in Eq. (4.1) to calculate these curves; the nonlocality parameter  $\beta$  has the conventional value of 0.85 fm.

curve, and the real part of the inversion potential was used for the 50 MeV (solid) curve. The points illustrating the ratio of the real parts of the two wave functions lie quite close to the Perey-Buck lines, but there is a noticeable discrepancy for the imaginary ratios, especially for the  $L = 0$  results. Nevertheless, the overall agreement with Eq. (4.1) is quite good, which indicates that the conventional Perey factor [Eq. (4.1)] appears to be adequate to represent the effect of the exchange nonlocality upon the wave function amplitudes, at least for the  $n\text{-}^{16}\text{O}$  example given here. This result is not sensitive to the details of the potential, because it was also found to hold for the case in which the density dependence was represented by one Gaussian only, as explained in connection to Eq. (3.2), and for which the inversion potential is illustrated by the “Inv-2” curve in Fig. 7. It would be of interest to extend this calculation to higher energies and heavier nuclei, especially because Owen and Satchler [16] find that the good agreement they obtained for the PDF with the Perey-Buck result for  $^{16}\text{O}$  becomes less good for the heavier nuclei. These results have an important negative implication: Having shown that the conventional Perey-Buck PDF represents the effect of the exchange nonlocality quite well and since channel coupling induces strong nonlocal effects [22,28], we conclude that it is *wrong* to suppose that the inclusion of a conventional Perey damping factor means that overall nonlocality has been adequately corrected for.

Comparison between the  $nl$  and  $l$  wave functions can also be carried out by doing an integral of physical sig-

nificance, containing one such wave function, and then comparing the integrals. Such a comparison has meaning for wave functions which are not phase equivalent. The integral chosen for this purpose is one which is akin to the ones which occur in the theory of the  $(e, e'p)$  reaction,

$$I_L = (kq)^{-1} \int_0^\infty \mathcal{F}_L(r) \exp(-2br^2) j_L(qr) dr. \quad (4.2)$$

Here  $q$  represents the momentum which the electron transfers to the nucleus, the spherical Bessel function  $j_L$  appears because the electron's incident and outgoing states are represented by plane waves, the exponential function represents the nuclear transition density, and  $\mathcal{F}_L$  is the distorted partial wave of the knocked-out nucleon in the final state, with outgoing momentum  $k$ . The two angular momentum numbers  $L$  should differ by the multipolarity of the transition, but this point is ignored. The results are illustrated in Figs. 11 and 12. In both figures the solid lines indicate the result for  $I_L^{(nl)}$  for which  $\mathcal{F}_L$  is the solution of the nonlocal Schrödinger equation with exchange. In Fig. 11 the dot-dashed line repre-

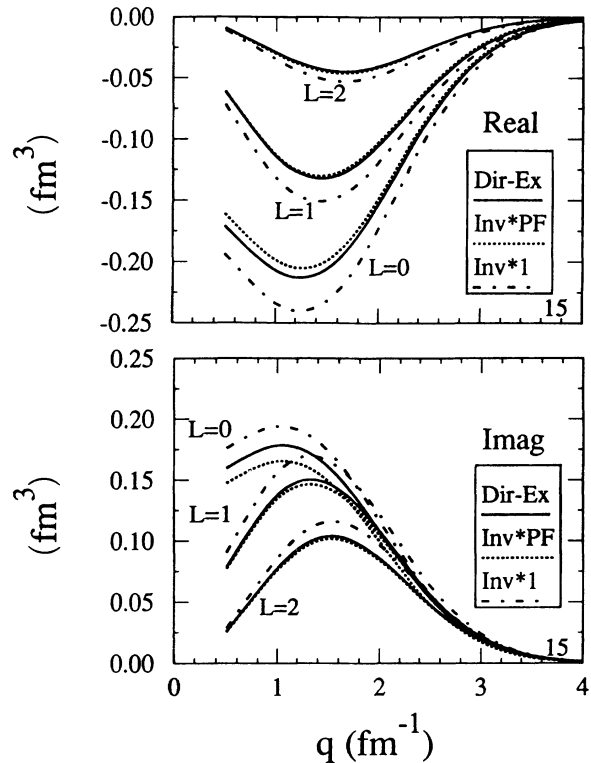


FIG. 11. Integrals of the type which occur in  $(e, e'p)$  calculations [Eq. (4.2)] as a function of the momentum transfer. The solid lines represent the results obtained with the exact nonlocal distorted wave function  $\mathcal{F}_L$ . When the wave distorted by the local inversion potential is used, one obtains the dotted and dot-dashed lines. The conventional Perey damping factor given by Eq. (4.1) was multiplied into the distorted wave for the dotted lines and was not used for the dot-dashed lines. The angular momentum number  $L$  for each partial wave is indicated next to the curves.

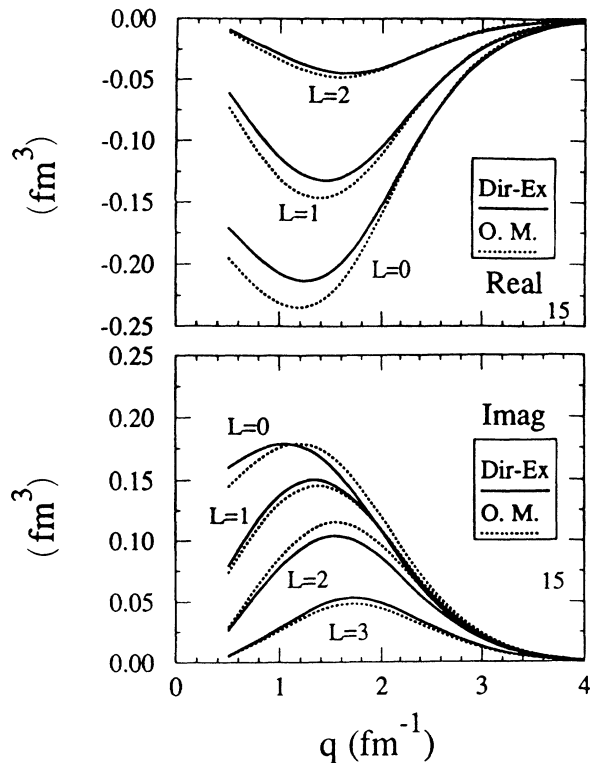


FIG. 12. Same as Fig. 11. The dotted lines are obtained when the distorted wave is calculated with the phenomenological optical potential of Ref. [26] and is multiplied by the conventional Perey damping factor of Eq. (4.1).

sents the value of  $I_L^{(l)}$  for which  $\mathcal{F}_L^{(l)}$  is the solution of the Schrödinger equation for the inversion potential, and the dotted curves are obtained by multiplying the same  $\mathcal{F}_L^{(l)}$  by the Perey damping factor of Eq. (4.1). For the low partial waves ( $L = 0$  and  $1$ ), the dot-dashed and dotted curves differ by about 16% which is compatible with the result that the local and nonlocal wave function amplitudes differ by 15% at small distances. The fact that the dotted lines are in good agreement with the solid ones is an indication that the conventional Perey damping factor is adequate in simulating the effect of the exchange nonlocality, at least for the partial waves higher than  $L = 0$ . The result for the phenomenological optical-model wave function, already multiplied by the PDF, is shown in Fig. 12. Here, however, a systematic difference with the exact nonlocal result of approximately 12% is found. Had the PDF not been used, then the optical-model result for  $I_L^{(l)}$  would have been larger than the nonlocal result by about  $16\% + 12\% \cong 28\%$ , at least for the real part of  $I_L$ , for the low partial waves. The effect on the  $(e, e'p)$  cross section would have still been larger since the latter involves the square of the matrix element of the type of  $I_L$ . Thus comparison between Figs. 11 and 12 illustrates the differences in the DWBA matrix elements when one uses a phenomenological versus a microscopic optical potential. However, as noted above, since our calculations do not include the dynamic polarization nonlocality, it

is doubtful whether the use of a PDF of the Perey-Buck type is justified.

## V. SUMMARY AND CONCLUSIONS

We obtained a rigorous  $L$ -independent local equivalent potential for  $n$ - $^{16}\text{O}$  scattering by a method of inversion, which represents the effects of the knock-on exchange nonlocality. This result should be useful for providing a comparison for approximate methods of obtaining LEP's. Our Sturmian method of obtaining the rigorous solution of the nonlocal Schrödinger equation requires the calculation of microscopic matrix elements which contain the wave functions of the two interacting nucleons. When the microscopic nucleon-nucleon interaction is given in terms of Gaussian functions, as is the case for the CEG interaction of Ref. [19] employed here, then these matrix elements (direct and exchange) can be calculated analytically [9]. By an inversion method [10], a local,  $L$ -independent "inversion" potential  $V_{\text{inv}}(r)$  was obtained from the SME's which is phase equivalent to the nonlocal Hartree-Fock potential. A comparison between the nonlocal and local phase equivalent wave functions shows that the decrease in the amplitudes of the nonlocal wave function compared to the local one is in reasonably good agreement with the conventional Perey factor given many years ago [2]. This result has been established so far only for the  $n$ - $^{16}\text{O}$  case, and it represents only the effect of the knock-on exchange nonlocality. The present results are based on the microscopic CEG effective nucleon-nucleon interaction [19]. Other interactions should also be tried, and different targets at different scattering energies should be explored, in order to establish more generally the results mentioned above.

The present work exemplifies a viable procedure whereby theories of scattering can be tested. Where there exists a reliable local phenomenological potential, one may exhibit the strengths and weaknesses of a nonlocal theory by comparing its local equivalent, determined by inversion, with that phenomenological potential. Although the present calculations have not included spin, the inversion procedure can be and has been applied where spin is included.

In addition to the exchange effect, another source of nonlocality is the dynamic polarization of the nucleus during the scattering process. The latter is as yet only poorly known. In two related studies, the inversion potential which represents a channel-coupling nonlocality was obtained [22,28] and the Perey damping factor was found to be quite different from the conventional Perey-Buck [2] result in that it generally is larger than unity and strongly angular momentum dependent. It seems to us surprising that the conventional Perey-Buck damping factor, which is based on the energy dependence of the phenomenological optical potential and hence should include the effect of all the nonlocalities, so closely resembles the damping due to exchange nonlocality alone. When both the channel-coupling and exchange effects are included simultaneously, then the Perey damping factor is not known, although the indications are that a cancel-



lation between the two effects takes place [29]. Further work along these lines would be desirable.

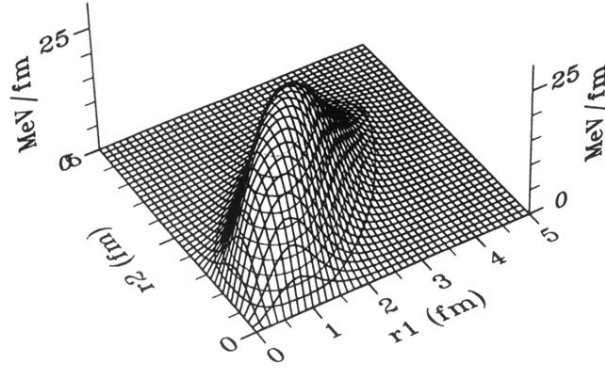
### ACKNOWLEDGMENTS

Thanks are due to Dr. Shinichiro Yamaguchi for considerable help with the CEG potential and with exchange

effects in general, to Dr. Jim Carr at FSU for comments concerning the calculation of local optical potentials from a density-dependent microscopic effective  $n$ - $n$  interaction, and to Dr. D. Onley and Dr. G. Wright for helpful comments concerning the  $(e, e'p)$  reaction, which led to the choice of the integrals  $I_L$  discussed herein. We are also grateful to the SERC, U.K., for support of Dr. Cooper. Finally, the excellent support from the computing center at UCONN is also much appreciated.

- 
- [1] F. G. Perey and B. Buck, Nucl. Phys. **32**, 353 (1962); N. Austern, Phys. Rev. **137**, B752 (1965).
- [2] F. G. Perey, in *Direct Interactions and Nuclear Reaction Mechanisms*, edited by E. Clementel and C. Villi (Gordon and Breach, New York, 1963), p. 125, Eq. (2).
- [3] L. B. Weinstein *et al.*, Phys. Rev. Lett. **64**, 1646 (1990); M. Waroquier *et al.*, Phys. Rep. **148**, 249 (1987).
- [4] D. Slanina and H. McManus, Nucl. Phys. **A116**, 271 (1968); F. Petrovich *et al.*, Phys. Rev. Lett. **22**, 845 (1969); J. W. Negele and D. Vautherin, Phys. Rev. C **5**, 1472 (1972); D. W. L. Sprung, M. Vallieres, X. Campi, and Che-Ming Ko, Nucl. Phys. **A253**, 1 (1975); M. Kohno and D. W. L. Sprung, *ibid.* **A397** (1983).
- [5] B. Sinha, Phys. Rep. C **20**, 1 (1975); B. Z. Georgiev and R. S. Mackintosh, Phys. Lett. **73**, 250 (1978); F. Petrovich, J. A. Carr, R. J. Philpott, and A. W. Carpenter, Phys. Lett. B **207**, 1 (1988).
- [6] H. Horiuchi, Prog. Theor. Phys. **64**, 184 (1980).
- [7] G. Rawitscher, Phys. Rev. **25**, 2196 (1982).
- [8] G. H. Rawitscher, J. Comput. Phys. **94**, 81 (1991).
- [9] D. Lukaszek and G. H. Rawitscher, Bull. Am. Phys. Soc. **36**, 2126 (1991); D. Lukaszek, Ph.D. dissertation, University of Connecticut, 1994.
- [10] R. S. Mackintosh and A. M. Kobos, Phys. Lett. B **116**, 95 (1982); S. G. Cooper and R. S. Mackintosh, Inverse Problems **5**, 707 (1989).
- [11] M. Lassaut and N. Vinh Mau, Nucl. Phys. **A349**, 372 (1980).
- [12] H. Fiedeldey, S. A. Sofianos, and L. J. Allen, Phys. Rev. A **32**, 3095 (1985).
- [13] T. Kaneko, M. LeMere, and Y. C. Tang, Phys. Rev. C **44**, 1588 (1991); **45**, 2409 (1992).
- [14] H. Horiuchi, Prog. Theor. Phys. **64**, 184 (1980); K. Aoki and H. Horiuchi, *ibid.* **68**, 1658 (1982).
- [15] S. Ait-Tahar, R. S. Mackintosh, S. G. Cooper, and T. Wada, Nucl. Phys. **A562**, 101 (1993).
- [16] L. W. Owen and G. R. Satchler, Phys. Rev. Lett. **25**, 1720 (1970).
- [17] W. Bauhoff, H. V. von Geramb, and G. Palla, Phys. Rev. C **27**, 2466 (1983).
- [18] H. Fiedeldey, Nucl. Phys. **77**, 149 (1966); **A96**, 463 (1967); **A115**, 97 (1968); M. Coz, L. G. Arnold, and A. D. MacKellar, Ann. Phys. (N.Y.) **58**, 504 (1970); **59**, 219 (1970).
- [19] N. Yamaguchi, S. Nagata, and T. Matsuda, Prog. Theor. Phys. **70**, 459 (1983).
- [20] H. F. Arrelano, F. A. Brieva, and W. G. Love, Phys. Rev. C **41**, 2188 (1990); Ch. Elster, Taksu Cheon, E. Redish, and P. C. Tandy, *ibid.* **41**, 814 (1990); R. Crespo, R. C. Johnson, and J. A. Tostevin, *ibid.* **44**, R1735 (1991).
- [21] S. G. Cooper and R. S. Mackintosh, Nucl. Phys. **A511**, 29 (1990).
- [22] S. G. Cooper and R. S. Mackintosh, Phys. Rev. C **43**, 1001 (1991).
- [23] S. Ait-Tahar, S. G. Cooper, and R. S. Mackintosh, Nucl. Phys. **A542**, 499 (1992).
- [24] S. G. Cooper and R. S. Mackintosh, Open University Report No. OUPD9201, 1992.
- [25] *Handbook of Mathematical Functions*, edited by M. Abramovitz and I. Stegun (Dover, New York, 1965), Sec. 10.2.1,  $i_n(z) = (\pi/2z)^{1/2} I_{n+1/2}(z)$ .
- [26] J. S. Petler, M. S. Islam, R. W. Finlay, and F. S. Dietrich, Phys. Rev. C **32**, 673 (1985).
- [27] G. Fricke, J. Herberz, Th. Hennemann, G. Mallot, L. A. Schaller, L. Schellenberg, C. Piller, and R. Jacot-Guillarmod, Phys. Rev. **45**, 80 (1992).
- [28] H. Fiedeldey, R. Lipperheide, G. H. Rawitscher, and S. A. Sofianos, Phys. Rev. C **45**, 2885 (1992).
- [29] Y. L. Luo, Y. Iseri, and M. Kawai, Prog. Theor. Phys. **81**, 396 (1989).

Real Part,  $L=0$  20 MeV



Real Part,  $L=3$  20 MeV

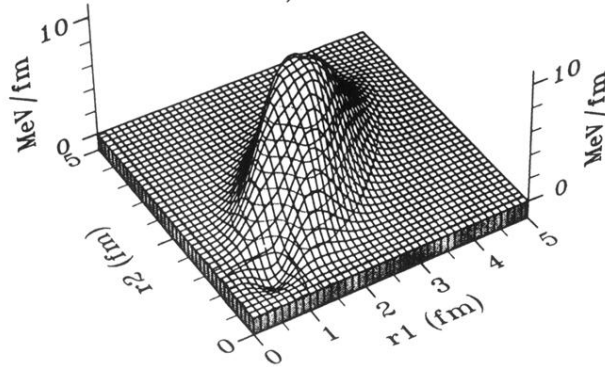
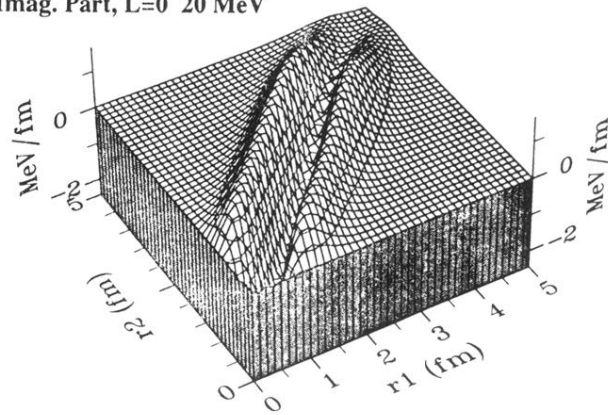


FIG. 1. Real part of the exchange kernel  $K_L(r_1, r_2)$ , defined by Eq. (2.3) for the  $n$ - $^{16}\text{O}$  interaction at an incident energy of 20 MeV. The microscopic  $n$ - $n$  interaction was taken from Ref. [19], with the imaginary part reduced by a factor of 0.6. The values of the angular momentum  $L$  are indicated. The change in the vertical scale between the top ( $L=0$ ) and bottom parts ( $L=3$ ) of the panels are to be noted.

Imag. Part, L=0 20 MeV



Imag. Part, L=3 20 MeV

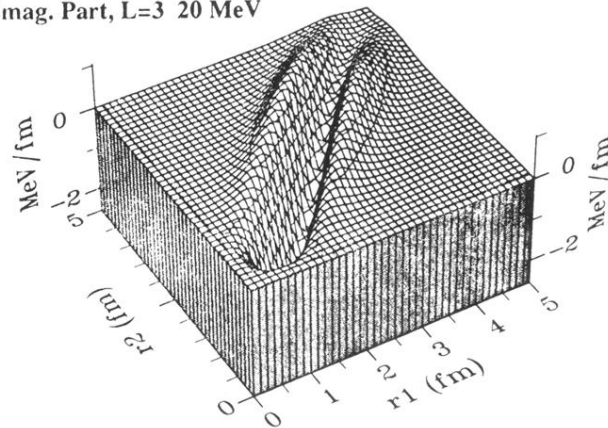


FIG. 2. Similar to Fig. 1 for the imaginary part of  $K_L(r_1, r_2)$ .

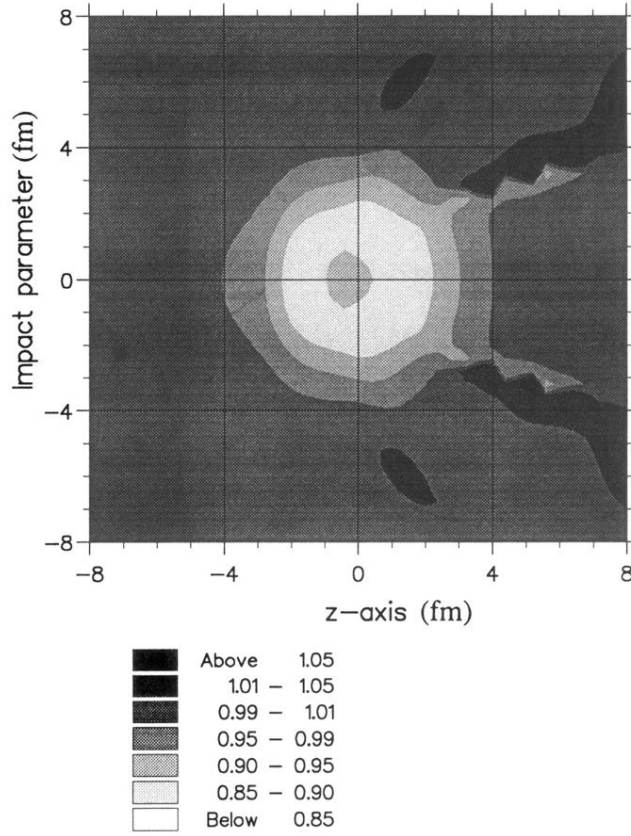


FIG. 9. Contour plot of the “total” Perey damping factor as a function of the impact parameter and the distance along the  $z$  axis for  $n$ - $^{16}\text{O}$  scattering at 20 MeV. This is the ratio of the absolute value of two “full” (summed over all partial waves) wave functions. The wave function in the numerator is the exact nonlocal one (with exchange); the wave function in the denominator corresponds to the local inversion potential. Near the center of the nucleus, this ratio lies between 0.90 and 0.95; in the next region, which is spread over most of the nuclear volume, the ratio is between 0.85 and 0.90. In the next two layers, it rises from between 0.90 and 0.95 to between 0.95 and 0.99. Outside of the nucleus, with the exception of a few bands at the right, the value of the ratio is between 0.99 and 1.01. The bands are due to the cumulative effect of a slight mismatch error in the asymptotic value of the wave functions.